THE INFLUENCE OF PILE SHAPE ON LATERAL LOAD RESISTANCE: FINAL SUMMARY REPORT #2 FOR STUDY TPF-5(272)

Prepared For:

Utah Department of Transportation
Research Division

Submitted By:

Brigham Young University
Department of Civil and Environmental
Engineering

Authored By:

Kyle M. Rollins
Dalin N. Russell
Guillermo Bustamante

**Final Summary Report #2
August 2018**

DISCLAIMER

The authors alone are responsible for the preparation and accuracy of the information, data, analysis, discussions, recommendations, and conclusions presented herein. The contents do not necessarily reflect the views, opinions, endorsements, or policies of the Utah Department of Transportation, the U.S. Department of Transportation, or other agencies that provided funding for the project. The Utah Department of Transportation makes no representation or warranty of any kind, and assumes no liability therefore.

ACKNOWLEDGMENTS

TECHNICAL REPORT ABSTRACT

1. Report No. UT-18.17	2. Government Accession No. N/A	3. Recipient's Catalog No. N/A	
4. Title and Subtitle THE INFLUENCE OF PILE SHAPE ON LATERAL LOAD RESISTANCE: FINAL SUMMARY REPORT #2 FOR STUDY TPF-5(272)		5. Report Date August 2018	
		6. Performing Organization Code N/A	
7. Author(s) Kyle M. Rollins, Dalin N. Russell, and Guillermo Bustamante		8. Performing Organization Report No. N/A	
9. Performing Organization Name and Address Brigham Young University Department of Civil and Environmental Engineering 368 CB Provo, UT 84602		10. Work Unit No. 4205315D	
		11. Contract or Grant No. 14-8434	
12. Sponsoring Agency Name and Address Utah Department of Transportation 4501 South 2700 West P.O. Box 148410 Salt Lake City, UT 84114-8410		13. Type of Report & Period Covered Final Summary Report #2 May 2014 – Aug. 2018	
		14. Sponsoring Agency Code PIC No. UT11.404	
15. Supplementary Notes Prepared in cooperation with the Utah Department of Transportation, the U.S. Department of Transportation, Federal Highway Administration, and other state DOTs on pooled fund study TPF-5(272)			

16. Abstract

The lateral resistance of pile foundations is typically based on the performance of circular piles even though other pile types are used. Due to a lack of data, there is a level of uncertainty when designing pile foundations other than circular piles for lateral loading. Theoretical analyses have suggested that square sections will have more lateral resistance due to the increased side shear resistance, but no test results have been available to substantiate the contention. Full-scale lateral load tests involving circular, square, and H piles were performed to consider the influence of soil-pile interaction on lateral load resistance. The load vs. deflection curves from the load tests show higher soil resistance from the H and square sections after accounting for differences in the moment of inertia for the different pile sections. The increased soil resistance can generally be accounted for using a p-multiplier approach with a value of approximately 1.25 for square piles or 1.2 for H piles relative to circular piles. This indicates that soil resistance on square and H piles is about 20% higher than that for round piles, and the increased resistance is primarily a result of increased passive resistance on the pile face rather than increased side shear. Alternative methods proposed to account for pile shape were not consistently reliable.

This is the Final Summary Report #2 for pooled fund study TPF-5(272), "Evaluation of Lateral Pile Resistance Near MSE Walls at a Dedicated Wall Site." Details of the research described in this report are available in the research final report prepared by Rollins et al. (2018) and published by the Utah Department of Transportation, along with the corresponding university theses.

17. Key Words Laterally loaded piles, circular pile, square pile, H pile, pile shape effect, p-multiplier, p-y curve, bridge abutments		18. Distribution Statement Not restricted. Available through: UDOT Research Division 4501 South 2700 West P.O. Box 148410 Salt Lake City, UT 84114-8410 www.udot.utah.gov/go/research	23. Registrant's Seal N/A
19. Security Classification (of this report) Unclassified	20. Security Classification (of this page) Unclassified	21. No. of Pages 47	22. Price N/A

TABLE OF CONTENTS

LIST OF TABLES

LIST OF FIGURES

UNIT CONVERSION FACTORS

SI* (MODERN METRIC) CONVERSION FACTORS

APPROXIMATE CONVERSIONS TO SI UNITS

Symbol	When You Know	Multiply By	To Find	Symbol
LENGTH				
in	inches	25.4	millimeters	mm
ft	feet	0.305	meters	m
yd	yards	0.914	meters	m
mi	miles	1.61	kilometers	km
AREA				
in^2	square inches	645.2	square millimeters	mm^2
ft^2	square feet	0.093	square meters	m^2
yd^2	square yard	0.836	square meters	m^2
ac	acres	0.405	hectares	ha
mi^2	square miles	2.59	square kilometers	km^2
VOLUME				
fl oz	fluid ounces	29.57	milliliters	mL
gal	gallons	3.785	liters	L
ft^3	cubic feet	0.028	cubic meters	m^3
yd^3	cubic yards	0.765	cubic meters	m^3
NOTE: volumes greater than 1000 L shall be shown in m^3				
MASS				
oz	ounces	28.35	grams	g
lb	pounds	0.454	kilograms	kg
T	short tons (2000 lb)	0.907	megagrams (or "metric ton")	Mg (or "t")
TEMPERATURE (exact degrees)				
°F	Fahrenheit	5 (F-32)/9 or (F-32)/1.8	Celsius	°C
ILLUMINATION				
fc	foot-candles	10.76	lux	lx
fl	foot-Lamberts	3.426	candela/m^2	cd/m^2
FORCE and PRESSURE or STRESS				
lbf	poundforce	4.45	newtons	N
lbf/in^2	poundforce per square inch	6.89	kilopascals	kPa

APPROXIMATE CONVERSIONS FROM SI UNITS

Symbol	When You Know	Multiply By	To Find	Symbol
LENGTH				
mm	millimeters	0.039	inches	in
m	meters	3.28	feet	ft
m	meters	1.09	yards	yd
km	kilometers	0.621	miles	mi
AREA				
mm^2	square millimeters	0.0016	square inches	in^2
m^2	square meters	10.764	square feet	ft^2
m^2	square meters	1.195	square yards	yd^2
ha	hectares	2.47	acres	ac
km^2	square kilometers	0.386	square miles	mi^2
VOLUME				
mL	milliliters	0.034	fluid ounces	fl oz
L	liters	0.264	gallons	gal
m^3	cubic meters	35.314	cubic feet	ft^3
m^3	cubic meters	1.307	cubic yards	yd^3
MASS				
g	grams	0.035	ounces	oz
kg	kilograms	2.202	pounds	lb
Mg (or "t")	megagrams (or "metric ton")	1.103	short tons (2000 lb)	T
TEMPERATURE (exact degrees)				
°C	Celsius	1.8C+32	Fahrenheit	°F
ILLUMINATION				
lx	lux	0.0929	foot-candles	fc
cd/m^2	candela/m^2	0.2919	foot-Lamberts	fl
FORCE and PRESSURE or STRESS				
N	newtons	0.225	poundforce	lbf
kPa	kilopascals	0.145	poundforce per square inch	lbf/in^2

*SI is the symbol for the International System of Units. (Adapted from FHWA report template, Revised March 2003)

EXECUTIVE SUMMARY

The lateral resistance of pile foundations is typically based on the performance of circular piles even though other pile types are used. Due to a lack of data, there is a level of uncertainty when designing pile foundations other than circular piles for lateral loading. Theoretical analyses have suggested that square sections will have more lateral resistance due to the increased side shear resistance, but no test results have been available to substantiate the contention. Full-scale lateral load tests involving circular, square, and H piles were performed to consider the influence of soil-pile interaction on lateral load resistance. The load vs. deflection curves from the load tests show higher soil resistance from the H and square sections after accounting for differences in the moment of inertia for the different pile sections. The increased soil resistance can generally be accounted for using a p-multiplier approach with a value of approximately 1.25 for square piles or 1.2 for H piles relative to circular piles. This indicates that soil resistance on square and H piles is about 20% higher than that for round piles. Therefore, design based on circular piles is conservative, while the use of appropriate p-multipliers could lead to increased efficiency. The increased pile resistance is primarily a result of increased passive resistance on the pile face rather than increased side shear. Alternative methods proposed to account for pile shape were not found to be consistently reliable. Therefore, the simple p-multiplier approach is preferred.

This is the Final Summary Report #2 for pooled fund study TPF-5(272), "Evaluation of Lateral Pile Resistance Near MSE Walls at a Dedicated Wall Site." Details of the research described in this report are available in the research final report prepared by Rollins et al. (2018) and published by the Utah Department of Transportation, along with the corresponding university theses.

1   INTRODUCTION

Until the mid-twentieth century, engineers knew relatively little about how to design deep foundations for lateral loads. It was generally assumed that deep foundations could only resist axial loads (Coduto, 2001). Since that time, case studies and theoretical models have proven that the same mechanisms that allow a pile to resist vertical loads are also engaged when a pile experiences lateral loads (Duncan,1994, Smith 1987). Although it is still a relatively new field of study, there are various methods available to compute the response of a pile to lateral load. Many of these methods are based on lateral load tests performed on circular piles. Square and H-Pile shapes are commonly used in practice but without much regard to shape effect. It is generally considered that the resistance of the square or H piles is equal to that of a comparable circular pile. Site specific tests are sometimes performed on various pile shapes to ensure that a specified resistance can be met, but no case study has been found in the technical literature which compares performance of piles with different shapes.

Briaud et al (1983) highlighted two major components of resistance that exist in a pile when it is vertically loaded and that are also present when it is laterally loaded. When a pile is loaded vertically, the pile derives its resistance from side friction and from the passive resistance or point bearing resistance at the toe. In the same way, when a pile is loaded laterally these same two components exist. The point bearing would be analogous to the passive resistance on the front face of the pile while the side friction would be analogous to the shear resistance on the sides of the pile. Because of differences in shape, both the passive resistance on the front face and the shear resistance on the side of a square pile might be expected to be larger than for those on a circular pile.

This principle is illustrated in Figure 1-1 as each pile shape is subjected to a lateral load shown as a green arrow coming from the left while being resisted by side shear forces, shown in red, and front facing passive forces, shown in blue. Notice, that as a round pile is loaded laterally the back half of the pile loses contact with the soil and therefore no shear resistance is developed on this surface. In contrast, three sides of a square pile remain in contact with the soil during lateral loading including longer side lengths to develop shear resistance. As a result, a square pile should have greater lateral soil resistance than a round pile of the same width. The H pile loaded about its weak axis may have about the same width and depth as the square pile therefore, it should develop similar side shear resistance. However, it should be noted that the moments of inertia of the various shapes are understandably different. In addition, to the differences in side shear, differences in passive resistance might be anticipated based on pile shape. For example, the normal force arrows for a square pile are all parallel to the direction of load while for a round pile the normal force arrows would have a component parallel and a component perpendicular to loading which might be expected to reduce lateral soil resistance. Like the bow of a ship through water, the shape of the round pile face can penetrate the earth easier therefore the effectiveness of the round pile in resisting lateral force will likely be less than that of a flat surface (Czerniak, 1957). Although an H pile loaded about its weak axis would also have a normal force arrow parallel to the applied load, there could be some differences in passive resistance owing to compression of the soil between the flanges.
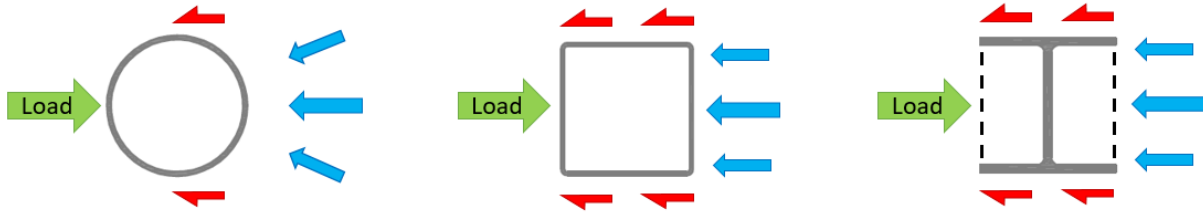
Figure 1-1: Shape influence on perceived stresses

To quantify these differences in geometry and soil-pile interaction, Reese and Van Impe (2001) proposed a method for calculating a larger equivalent diameter, b_{eq} for square cross sections. Other methods have also been devised to consider shape factors in lateral pile design. Czerniak (1957), explaining the overturning resistance of piles, detailed a reduction to allowable lateral earth pressure of 0.636 for circular piles relative to square piles. Using a pressuremeter based approach, Smith (1987) proposed a procedure that applied shape factors to compute side shear and passive resistance. In this approach, the ultimate side shear is computed using shape factors of 0.79 and 1.76, for circular and square shapes, respectively. Similarly, shape factors for the passive resistance are 1.0 for square piles and 0.75 for circular piles. These factors were an adjustment from earlier recommendations by Briaud et al. (1983) which suggested a passive resistance shape factor of 0.8 for circular piles, instead of 0.75, as well as a side shear shape factor of 2.0 for square piles and 1.0 for circular piles. Currently, there are no suggested shape factors for the design of H piles, although similar values might be used.

Although these concepts on the influence of pile shape seem correct conceptually, there is a lack of full scale test data that could verify the theorized methods. It is possible that this uncertainty is the reason why current lateral pile analysis programs, such as LPILE, do not apply a shape factor in calculations and only consider the shape's effect on the moment of inertia. Is

pile shape a contributing factor to overall lateral resistance? If it is, is the contribution worth including in pile design procedures? If included, would the consideration of pile shape save money on deep foundation projects?

This study aims to answer those first two questions, while leaving the discussion on pile economics primarily to the client and the engineer. This report provides a summary of full scale, lateral load tests on round, square, and H piles to determine the influence of pile shape on lateral load resistance. The piles tested had similar material properties with comparable dimensions and moments of inertia to allow for a direct comparison of lateral resistance. To provide a full view of the pile response, the experiment was documented with instruments that measure lateral deflection, lateral load, heave, pile rotation, and pile moment. As a method of analysis, the measured load tests where compared to current lateral design methods to gauge accuracy in predicting lateral resistance. The use of p-multipliers in an LPILE analysis provided a reasonable and consistent method for predicting the lateral resistance of square and H piles.

This is the Final Summary Report #2 for pooled fund study TPF-5(272), "Evaluation of Lateral Pile Resistance Near MSE Walls at a Dedicated Wall Site." Details of the research described in this report are available in the research final report prepared by Rollins et al. (2018) and published by the Utah Department of Transportation, along with the corresponding university theses.

2   TEST LAYOUT

An undeveloped area of land located between Bluffdale and Lehi, Utah was chosen for the test site (see Figure 2-1). The location can be found using coordinates 40°27'10.95" N 111°53'54.63" W. Access to the plot of land was provided by Geneva Rock who formerly used it as a gravel pit. This rather isolated location with granular native soil was a desirable site for testing.

Figure 2-1: Test Site Location (Google Earth 2013)

2.1 Piles Tested

To investigate the effect of pile shape on lateral load resistance, round, square and H piles were selected for testing. Table 2-1 provides a summary of the properties of the piles chosen for testing. There were two round 12.75X3/8" piles, three square HSS 12X1/4" piles, and one H shaped HP 12X74 pile used in testing. The pipe piles and square tube piles were donated by Atlas Steel while the H pile was donated by Spartan Steel. The tubular round piles conform to the American Society for Testing and Materials (ASTM) A252-10 GR 3 specification and have a yield strength of approximately 57 ksi. The non-compact H pile conforms to ASTM A572-50 specifications with a minimum yield strength of 50 ksi, while the steel of the square pile conforms to ASTM A500-10A Grade B&C specifications having a minimum yield strength of 46 ksi.

Piles of similar dimension were selected so that they could be relatively comparable in width despite differences in geometric shape. Although square steel tube piles are not common, steel was selected for this pile shape so that differences in pile-soil interface friction could be avoided. An H pile shape with a smaller cross sectional area, such as an HP 12x53, could have been used, however inelastic global buckling in the flanges would reduce the moment capacity by about 20%. The HP 12x74 shape was chosen for a theoretical capacity of 90% of the yield moment capacity so that failure in the soil could be observed before buckling in the pile became a concern. The piles were intended to act as a long pile, therefore the pile length of 40 ft was deemed an appropriate pile length with a length to width/diameter ratio (D/B) of nearly 40.

Table 2-1: Pile Properties

Type	Diameter/ Depth (in)		Wall Thickness (in)		Cross Sectional Area (in²)	Moment of Inertia (with angle iron) (in⁴)	E (ksi)	F_y (ksi)
Round 12.75X3/8	12.75		0.349		14.57	279 (314)	29,000	57
HSS 12x12X1/4	12		0.233		14.8	248 (335)	29,000	46
HP 12X74	12.1	12.2	0.605	0.61	22.6	186 (186)	29,000	50
	Flange Depth	Flange Width	Web Thickness	Flange Thickness				

Desert Deep Foundations, Inc. used an ICE I-30V2 diesel hammer to drive the test piles 18 ft into native soil. The tubular piles were driven open ended which resulted in a soil plug with a length of 10.4 ft to 12.1 ft above the toe of the pile. The piles were left hollow so that the non-linear behavior of a cracked concrete fill did not have to be considered which better facilitates back analysis using the program LPILE. After the piles were driven, granular backfill was compacted around the test piles first to an elevation of 15 ft and then to an elevation 20 ft above the native soil surface. This left about 2 feet of pile above the ground surface.

2.2   Backfill Material

The backfill was a silty sand with gravel that classified as an SM material according to the Unified Soil Classification System and as an A-1-a material according to the AASHTO classification system. A typical grain-size distribution curve is plotted in Figure 2-2.
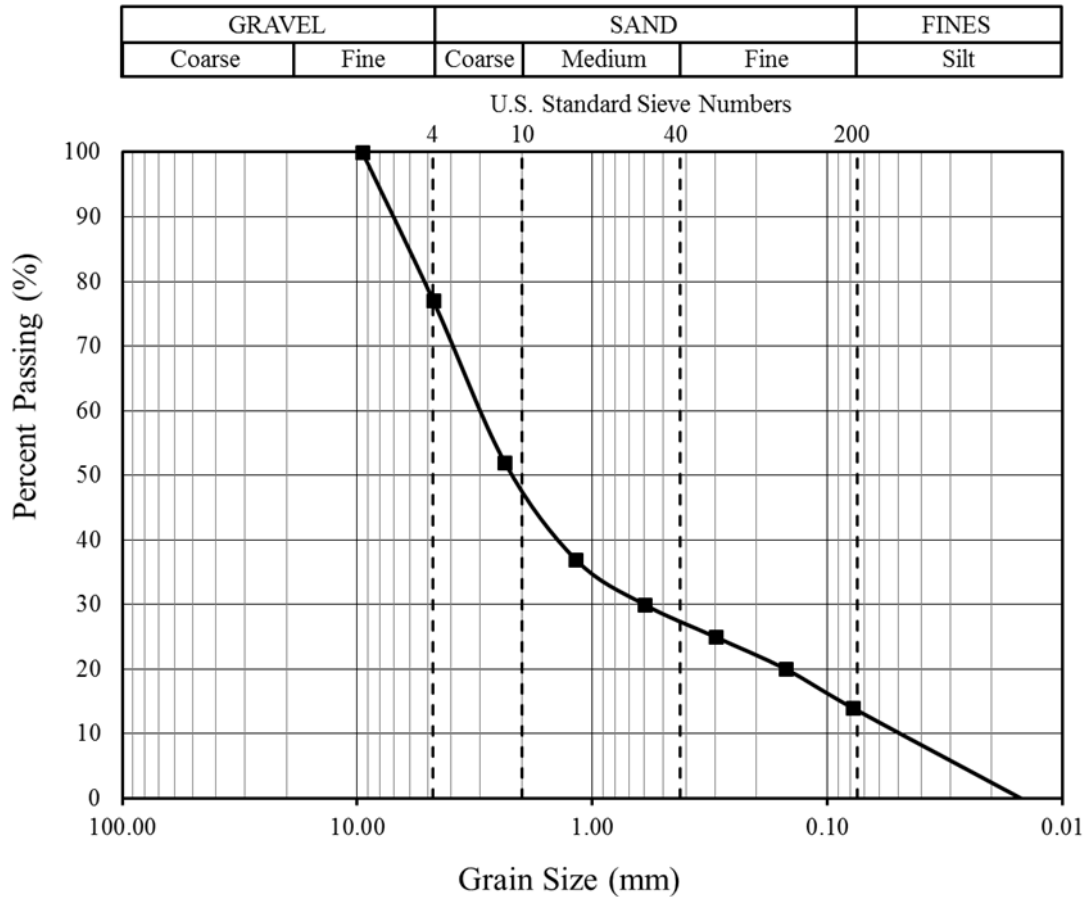
Figure 2-2: Particle Size Distribution Curve for Selected Backfill

Based on this curve, the mean grain size (D_{50}) is 2.3 mm, the coefficient of gradation (C_c) is 1.6, the coefficient of uniformity (C_u) is 40, and the fines content is 14%. A standard Proctor test produced a maximum density of 126.7 pcf and an optimum moisture content of 7.8%. Further information on this backfill material can be found in subsequent sections explaining the compaction of the backfill.

There were three phases of soil compaction at this test site. An explanation of each of these phases is provided in this section. The initial phase of soil compaction consisted of 15 ft of backfill material to be compacted on top of the native soil. This material was placed in 12-inch lifts and compacted by a vibratory roller compactor. The material was moisture conditioned to

sustain optimum levels throughout compaction. Lateral load tests on four piles were performed at this level including two square, one round, and one H pile. The first test was performed by reacting a round pile against a square pile while the second test reacted another square pile against an H pile.

The second phase of soil compaction added five more feet of backfill on top of phase 1 reaching 20 ft of backfill over the native soil. A load test between a round and an H pile was performed in phase 2 compaction. Similar to the compaction in phase 1, phase 2 used a vibratory roller compactor with 12-inch lifts as shown in Figure 2-3. In phase 1 and 2, a jumping jack type compactor was used to compact immediately around the test piles where the roller could not fit, such as between the two piles within close proximity to each other as shown in Figure 2-3. The material in phase 2 was moisture conditioned, as shown in Figure 2-3, to achieve optimum moisture conditions.

Figure 2-3: Phase 2 Compaction

Phase 3 was a recompaction phase which allowed the re-testing of two piles, a round pile and a square pile, in virgin soil conditions. A procedure was designed to effectively remove any disturbed soil from previous tests and place re-compacted soil in the direct zone of influence around the piles to be re-tested. Based on technical literature (Duncan et al., 1994) and results from the tests done in phase 2, it was decided that the majority of lateral pile resistance would be developed within the top 6 ft of the soil profile at this site. A pit measuring 6 ft wide, 6 ft long and 6 ft deep was excavated around the two piles on the side in the direction of loading. Because of the size of the pit, a jumping jack compactor had to be used for compaction. To promote uniformity between phases of compaction, phase 3 re-compaction was performed with 6-inch lifts rather than 12-inch lifts because of the limited zone of influence of a jumping jack compactor. Special effort was made to provide compactive energy in the immediate vicinity around the piles where compaction is likely to have significant effects on lateral resistance at small deflection levels.

Nuclear density tests were performed to check conformity to at least 95% of the standard proctor dry density and near optimum moisture content. Based on these measurements, the moisture content, dry unit weight, calculated moist unit weight and relative compaction of the measured soil properties for phase 2 and phase 3 are shown in Table 2-2. The overall average, standard deviation, and coefficient of variation have been calculated and are also reported in this table.

Table 2-2: Measured soil properties during each phase of compaction

Phase of Soil Compaction	Moisture Content (%)	Dry Unit Weight (pcf)	Moist Unit Weight (pcf)	Relative Compaction (%)
1	6.0	122.8	130.1	96.4
2	7.0	122.9	131.5	97.0
3	6.1	121.9	129.3	96.3
Average	6	123	130	97
Standard Deviation	0.56	0.53	1.09	0.39
Coefficient of Variation	0.09	0.004	0.01	0.004
Optimum	9.7	126.7	139	95

Although these measurements indicate that the soil densities are relatively uniform throughout the test site, the extent of this data should be explained. The nuclear density gauge was set to depths of 6 to 8 inches during density testing. While this ensures that the phase 3 data, which was compacted in 6-inch lifts, is uniform, it can introduce a degree of uncertainty for the phase 1 and phase 2 data, which was compacted in 12-inch lifts. The compaction data for the phase 2 tests reports satisfactory compaction results although this data is only representative of the depth to which the soil was tested. It is possible that at depths below that which was tested, from 8 to 12 inches, lower levels of compaction were obtained. It is common practice to use a roller compactor for 12-inch lifts, although in smaller areas where a jumping jack compactor was used for a 12-inch lift, there is a higher probability that lower compaction may have occurred at greater depths. The moisture conditioning was applied in a uniform manner throughout all the layers, and the moisture content of the material was kept within an acceptable range to provide sufficient compaction in the regions that were tested.

Various data collection methods were used during the load tests to record the magnitude of the load applied, deflection of pile, pile rotation at head, ground heave, deflection at the ground

surface and strain along the length of the pile. These observations were critical toward explaining

pile performance and for making comparisons between the individual piles. The subsequent

sections explain the instrumentation used during each test.

2.3   Load Cell and Pressure Transducers

The load applied during each test was recorded by a strain gauge cell as well as an

electronic pressure transducer in line with the hydraulic pump. The cell was located immediately

in front of the hydraulic jack as it transferred the load from the hydraulic pump to the piles. A

variety of steel struts were used to span the distance between test piles. During testing the load

was verified with the pressure transducer which measured the hydraulic pressure from the

hydraulic jack. Figure 2-4 provides a photo showing the load cell, jack and strut set-up between

two test piles. To eliminate the buildup of a moment at the load point, the loading strut was

pinned to a clevis on one pile while two spherical end platens were located on the opposite pile

for the same purpose, which ensured safety in testing. Measurements were recorded by a

Megadac computer data acquisition system at a rate of two readings per second. The same

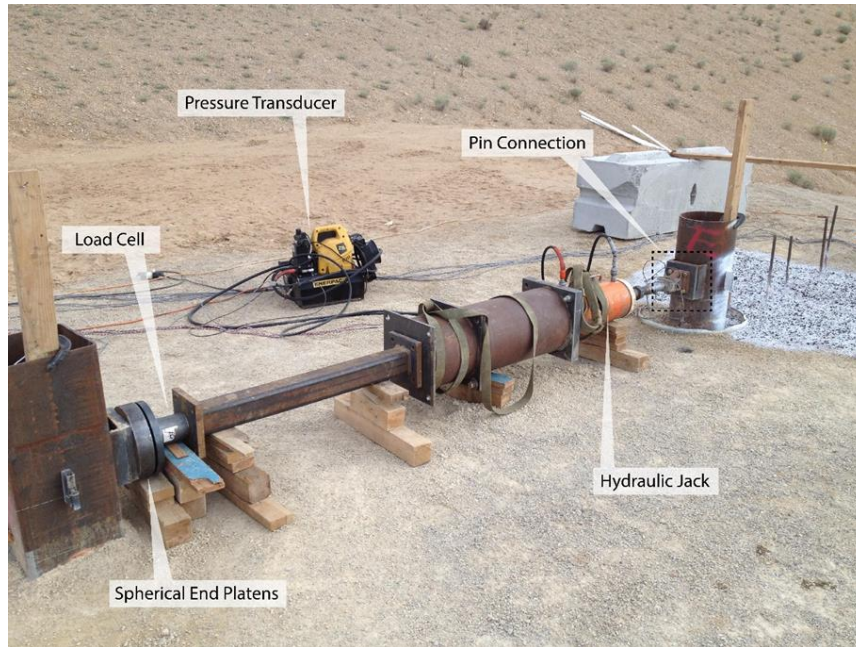instrumentation procedure was used in all of the tests.

Figure 2-4: Load Test Arrangement

2.4   String Potentiometers

The displacement and rotation of the pile as well as the displacement of the ground surface immediately around the pile were measured using string potentiometers or string pots, as shown in Figure 2-5. Independent reference frames were constructed out of two pre-cast concrete blocks weighing around 3600 lbs spaced at about 8 ft on either side of the test pile. The string potentiometers were attached to this reference frame as well as their different points of observation. The pile head displacement was recorded by attaching a string potentiometer to a location on the pile one foot above grade using a magnetic clip. This was also the elevation at which load was applied. Another string pot was fixed to the pile at a location three feet above the load point to measure pile deflection. Pile rotation could then be computed by taking the difference in lateral deflection between the two points and dividing by the vertical distance between them.

14

Stakes were placed in the ground at measured increments from the pile with string potentiometers attached in order to measure ground surface displacement. Figure 2-5 (left) shows how the string potentiometers were set up for the first test. During a few of the first tests the lateral deflection reading at the first stake, closest to the pile, showed inconsistent results. As failure planes propagated through the soil, this stake had a tendency to rotate toward the pile, giving false deflection readings. A new system using a metal plate with three small pins at the bottom driven in the ground and one upright stake to hold the string line proved a more efficient way to measure lateral ground deflection.
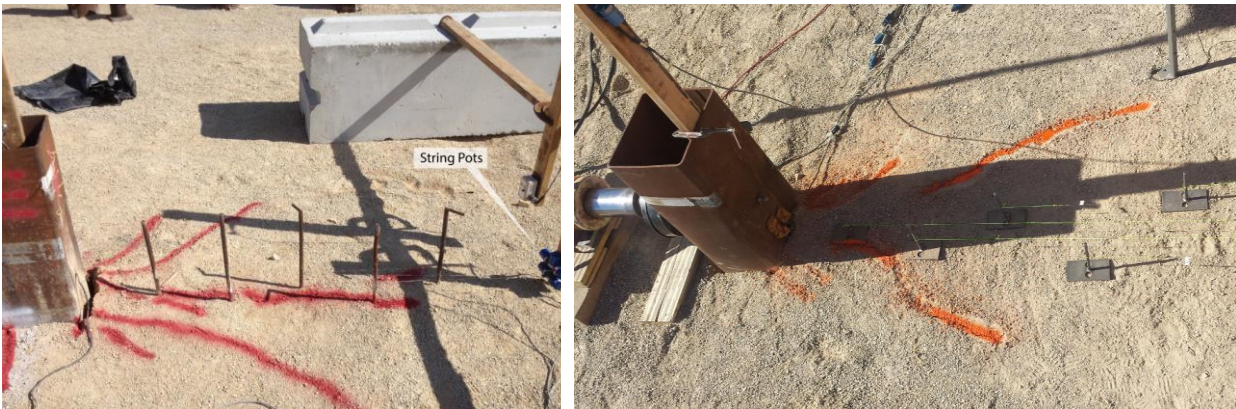
Figure 2-5: String Potentiometers in Place during Testing

2.5 Strain Gauges

To calculate pile moment with depth, waterproof electrical resistance type strain gauges were installed along the length of each pile prior to driving. In order to protect the gauges during driving, the line of strain gauges was covered with a steel angle which was tack welded to each pile between strain gauge locations. The strain gauges were placed on the pile at depths of 2, 4, 6, 9, 12, 15 and 18 ft below the ground surface. Two strain gauges were placed at each depth on

opposite exterior sides of the pile and in line with the direction of loading. This allowed the collection of strain measurements on the pile as the pile face was subjected to tension or compression during loading. Strain gauges were placed on the web of the H pile, whereas the square round pile had strain gauges on the face of the pile in line with loading. Trial readings were taken beforehand to calibrate the data collection system to the strain gauge readings.

2.6   Digital Image Correlation Camera System

Relatively little information is available in the literature regarding ground heave and displacement patterns in soil adjacent to a laterally loaded pile. To better capture the ground displacement around the piles during lateral loading, both Digital Image Correlation (DIC) equipment and conventional surveying equipment were used. A survey level provided heave measurements along a line in the direction of loading from the pile face at one foot intervals to a distance of five feet. In contrast, the DIC equipment provided displacement information at thousands of points of points in an large area in front of the test pile. The DIC method was used in this study to provide detailed measurements of ground heave around the piles during loading. This appears to be the first application of this technology for this purpose. The DIC system, manufactured by Dante Dynamics, collects data by using two digital cameras placed at a known height from the ground and spaced at a fixed distance apart from each other. The cameras were oriented so that their line of sight overlapped with the companion camera creating a field of vision approximately 8 ft x 6 ft. Corresponding shots were taken by each camera of the same object at the same time. The analysis software then used a correlation algorithm to recognize displacements of thousands of points in the x, y and z direction. With this information, color contour plots can be generated of displacement, deformation, and strain. The setup of the data collection system in this test is shown in Figure 2-6. Ground heave was expected on the side of

16

the piles opposite to the loading, and the DIC cameras were installed to measure the deformation of the ground in that area. Objects with a high contrast pattern provide the most accurate data, so the ground was painted white to contrast against the black painted gravel that was arranged in the camera view. The system is sensitive to measurements down to 1/100,000 of the field of view (Measurement Principles of DIC). This setup resulted in a calculated measurement uncertainty of three thousandth of an inch (0.003 in). Digital images were taken immediately after each load increment during the test and again after a five minute hold period.
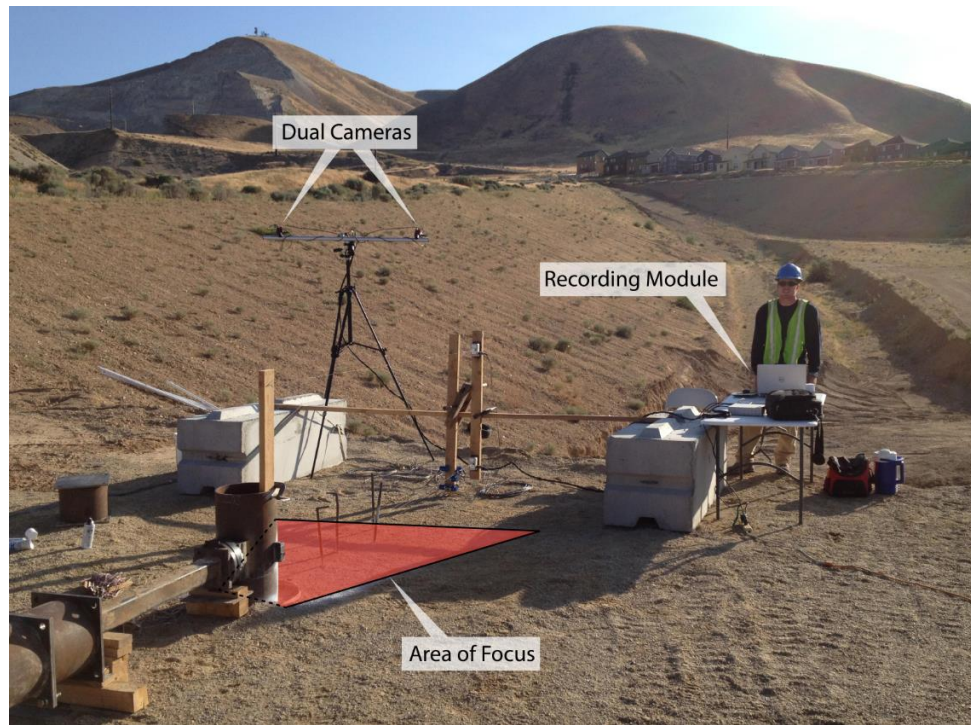

Figure 2-6: Test Apparatus with Independent Reference Frame and DIC Cameras

3   **LATERAL LOAD TESTING**

Lateral pile deflection measurements were taken at 1 foot above the ground. This was also the point where the load was applied and can be referred to as the pile head. These measurements at the pile head were used to create pile head load versus displacement curves for the various load tests. Each curve is based on the average load and displacement readings over a 30 second interval one minute after the peak load. The peak load, which might be more appropriate for dynamic loading conditions, was about 5% higher. These curves provide a basis by which to compare the lateral resistance of each pile shape. Pile head load vs. deflection curves for the phase 1, 2, and 3 tests are presented in Figure 3-1, Figure 3-2, and Figure 3-3.

A comparison of the load-deflection curves for phase 1 (Figure 3-1) with 15 ft of fill indicates that the resistance is lowest for the H pile for a given deflection. This was expected because the load was applied perpendicular to the web (weak axis) of the H pile, where the moment of inertia is about 40% lower than the square pile and circular pile. Many transportation departments reportedly use weak axis orientation for H piles in integral abutment bridges (Filz et al., 2013). Nevertheless, the reduction in resistance is not as great as might have been expected as discussed subsequently. Although the moment of inertia and width/diameter are very similar for the square and circular piles, the square piles show more resistance to lateral loading than the circular pile. The square piles typically had lateral resistance that was 10 to 20% higher than the round pile for a given deflection. The consistency of the results for the two square piles suggest that the sand density was consistent over the site as indicated by nuclear density testing.

For the Phase 2 tests (Figure 3-2) with 20 ft of backfill soil and one foot lifts, the load-deflection curve for the round pile is very similar to that for the Phase 2 tests, confirming the consistency of the results. Once again the load-deflection curve for the H pile is lower than that

for the round pile as expected. However, the resistance for H pile in the Phase 2 test is somewhat lower than that for the Phase 1 tests. This is could be a result of variation in soil compaction between the flanges. Compaction in this narrow zone is relatively difficult to accomplish.

For the Phase 3 tests (Figure 3-3) with 20 ft of backfill soil and 6-inch lifts, the load-deflection curves for the square and round piles are significantly higher than comparable curves from Phase 1 and Phase 2. These results suggest that the density of the backfill is higher in these tests likely owing to the thinner lifts and greater uniformity of compaction as discussed previously. Despite the higher density, the load-deflection curves for the two square piles are consistent and show a 15 to 20% increase in resistance relative to the round pile. These results are consistent with observations from Phase 1 testing
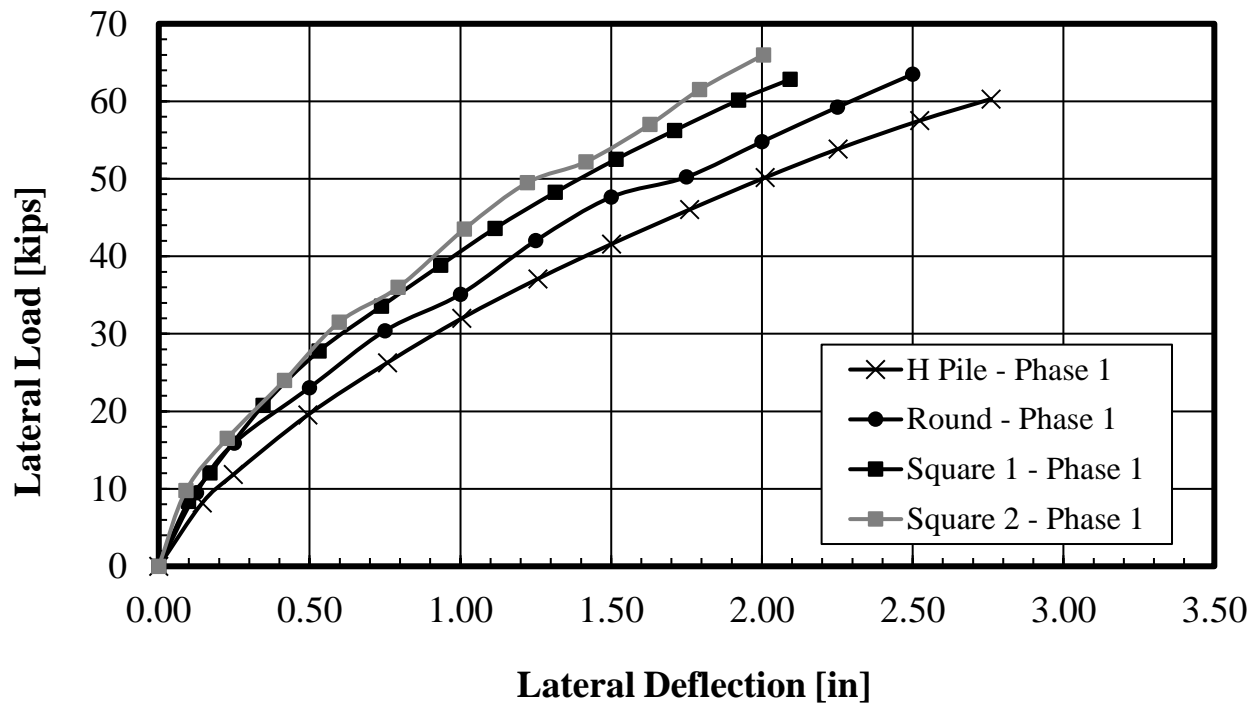

Figure 3-1: Pile head lateral load-deflection curves for square, H and round piles tested during Phase 1.
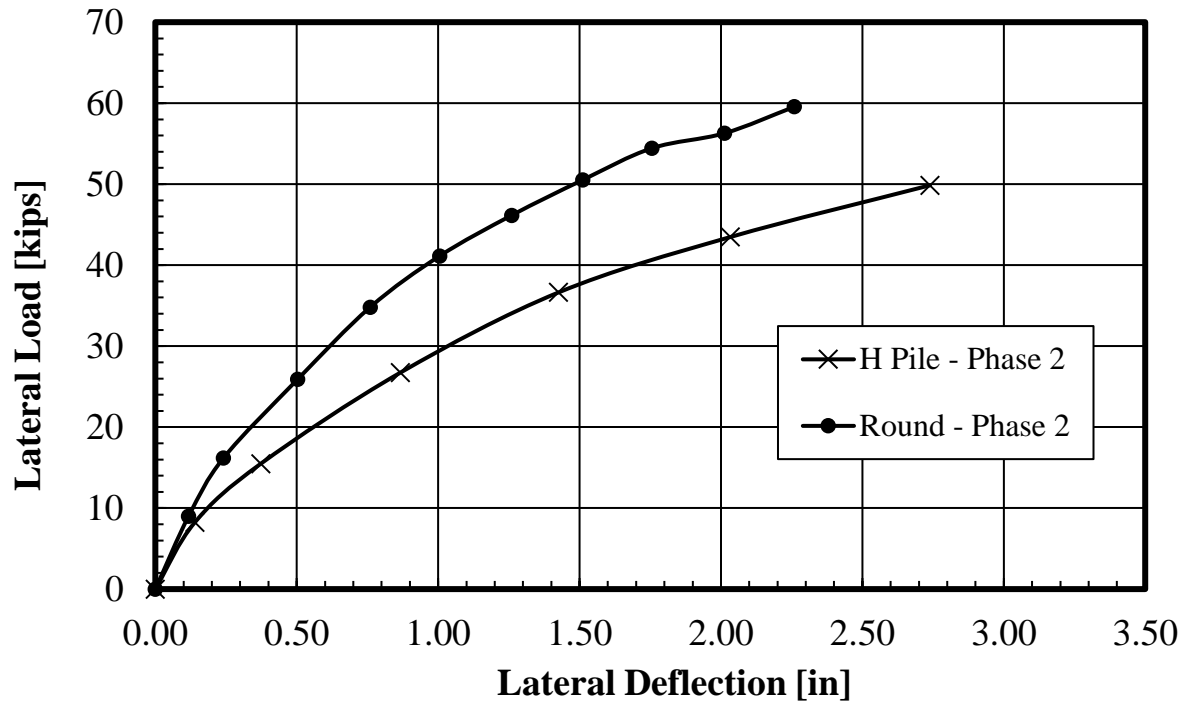
Figure 3-2: Pile head lateral load-deflection curves for H and round piles tested during Phase 2.
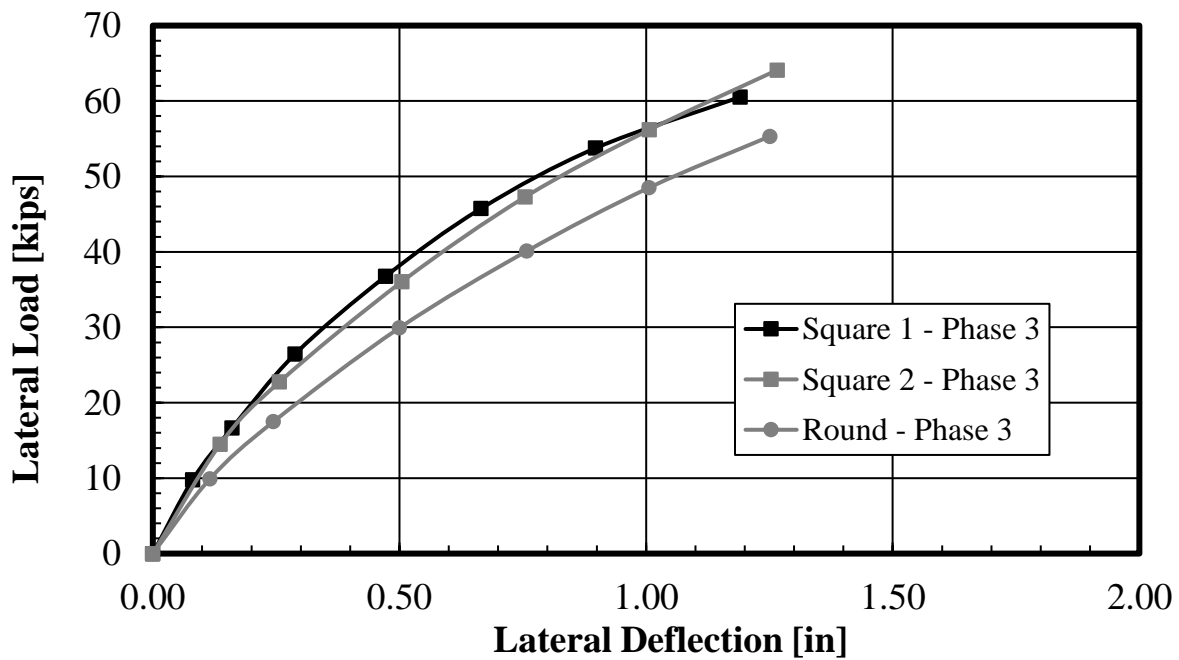

Figure 3-3: Pile head lateral load-deflection curves for square and round piles tested during Phase 3.

3.1 Shear Plane Development During Lateral Loading

After completion of each lateral load test, the cracks and shear planes that developed on the ground surface in front of the pile were spray painted for better observation and recording of the failure surfaces. Measurements of the cracks and angle with respect to the edge of the pile were taken. Figure 3-4 shows comparative pictures of the failure planes for the three different pile shapes. The square and H pile developed trapezoidal wedge type failures, while the failure geometry for the circular pile was more elliptical. Failure planes are very distinct and develop at the corners for the square and H piles, while the failure planes are more dispersed around the perimeter of the round pile.

Pile Type: HP12x74
Failure Geometry: Wedge
South Crack Length: 35.3 cm
North Crack Length: 32.3 cm
Angle South: 38°
Angle North: 45°

Pile Type: HSS12x1/4
Failure Geometry: Wedge
South Crack Length: 45.7 cm
North Crack Length: 47.2 cm
Angle South: 34°
Angle North: 36°

Pile Type: 12x3/8
Failure Geometry: Elliptical
South Crack Length: - cm
North Crack Length: - cm
Angle South: --°
Angle North: --°
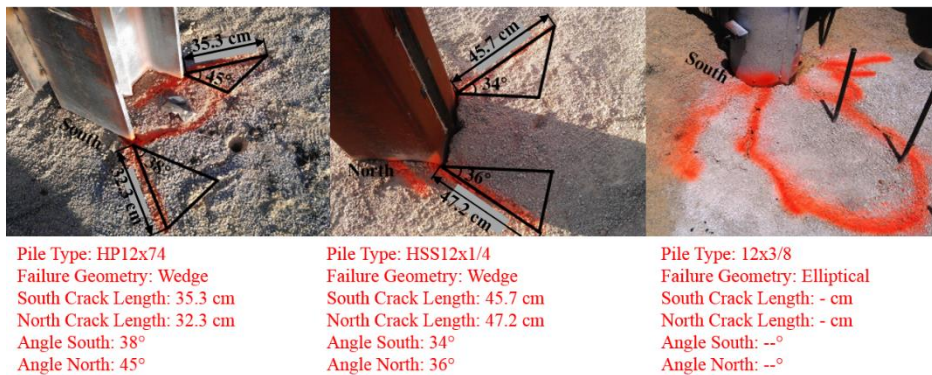
Figure 3-4: Shear planes adjacent to each pile shape at end of lateral loading.

Reese and Van Impe (2001) suggest that failure planes fan out from the edge of square shaped piles at an angle, α, between ϕ and ϕ/2 for dense sand, where ϕ is the soil friction angle. As discussed subsequently, the friction angle for the sand is about 45°, and the measured α values are typically about 80% of ϕ which is in good agreement with expectations for dense sand.

3.2 Lateral Ground Displacement

As the pile was loaded during each test, pressure would transfer to the surrounding soil causing the soil to displace. The lateral displacement of the ground at certain distances from the pile was measured using string potentiometers attached to stakes in the ground. These measurements help determine how lateral pile loading affects the ground around it and the extent of the failure wedge that is produced.

In certain applications it is important to know how a laterally loaded pile will affect surrounding objects such as other piles in a pile group or spread footings. Based on test measurements, a normalized deflection versus normalized distance plot was developed as shown in Figure 3-5 for cases where the pile experienced 0.25, 0.5 and 1.0 inches of deflection at the pile face. While there is some variation with pile shape and pile deflection, the general trend is consistent for all tests. A best fit curve based on all the data is given by the equation

$$\delta = 0.0042d^4 - 0.0548d^3 + 0.276d^2 - 0.7125d + 1.0 \tag{3-1}$$

where d = distance from the pile face in pile diameters and δ = horizontal ground displacement as a percentage of displacement at the pile face. This equation which is also shown in Figure 3-5 yields an R^2 value of 0.98 indicating a very strong correlation in the response. Equation 3-1 can be used to estimate the ground deflection as a function of distance from the pile face according to pile diameter and expected deflection at the pile face. Alternatively, if ground deflection limits are known at some distance, this curve can be used to estimate the pile head deflection limit that would be required for a given pile diameter. It should be noted that these curves are for sands at a 96% relative compaction, so differences might occur for looser sands. Interestingly, the

agreement in the data as a whole suggests that pile shape does not influence the magnitude of ground displacement in front of a pile being loaded.

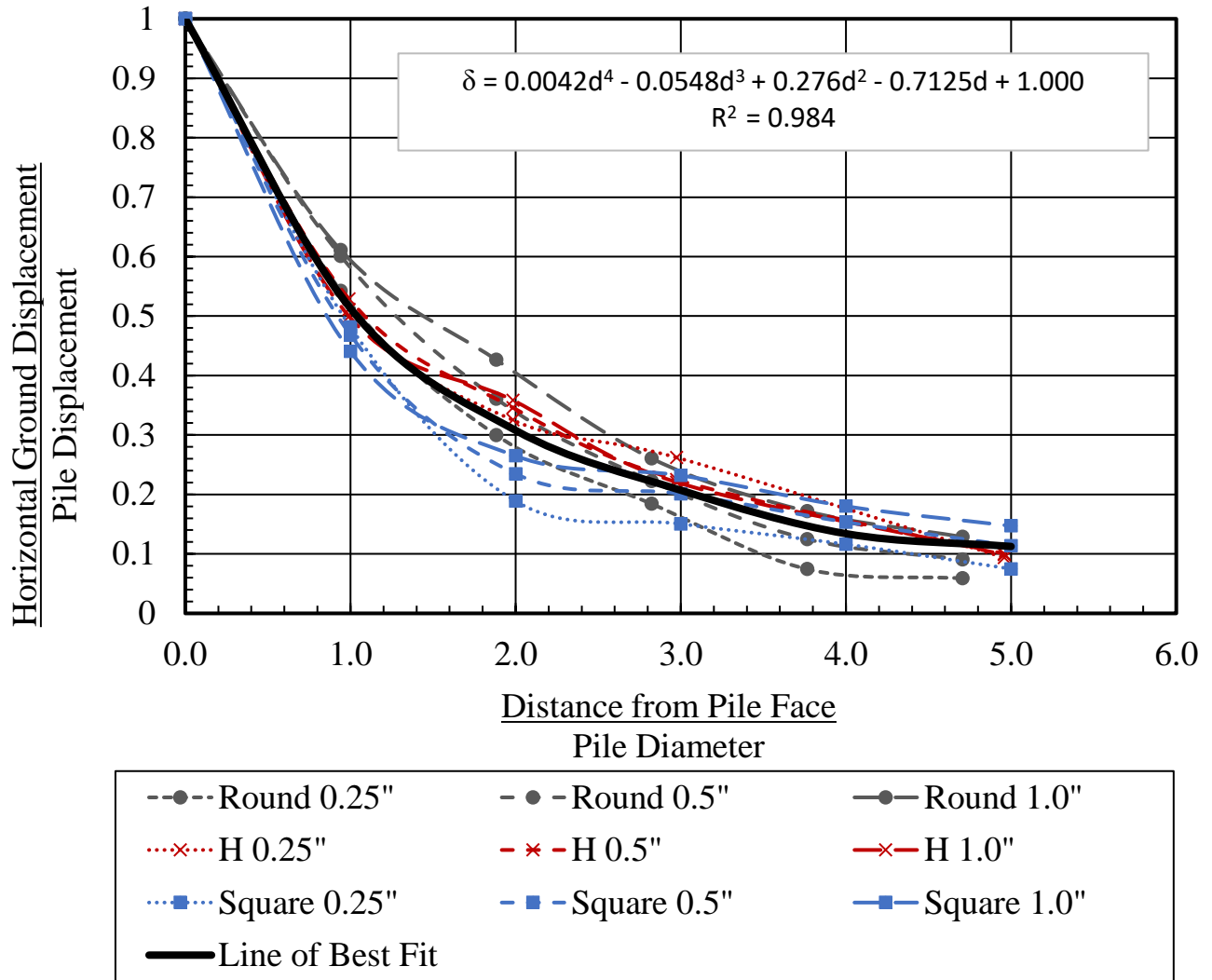**Figure 3-5: Normalized lateral ground deflection versus normalized distance from pile face.**

3.3 Ground Heave

As each pile deflected laterally under the applied load, the compacted soil around the pile would also displace vertically, like rubber being squeezed in one direction expands in the other. Measurements of this vertical displacement, or heave, at a distance from the pile can indicate the

zone of influence in front of the pile itself. This information can influence the design of pile groups, bridge abutments, or structures near deep foundations. With the use of a level survey and DIC cameras, measurements were collected to observe this phenomenon and determine how it might change for different pile shapes. A common trend among these plots is that ground heave is greatest at the pile face and slopes down to near zero at a distance of around 4 to 5 pile diameters (or 4 to 5 feet in this case) from the pile face.

Combining the heave data from the DIC and survey measurements into one plot facilitates further comparisons concerning pile type and heave. A fair comparison between pile types must consider the diameter or width of the effective pile as well as the overall heave. Figure 3-6 presents this comparison as normalized heave (heave at any distance divided by heave at the pile face) plotted against normalized distance (distance from the pile face divided by pile width or diameter). In this plot, survey measurements for the round and H pile data are matched with the DIC readings of the square piles which a provide more detailed heave profile for these shapes. The H pile was oriented about its weak axis therefore flange ends where considered as the effective pile face. Based on the normalized heave curves, there is very good agreement between ground heave produced by the round, square and H piles. This result suggests that there is relatively little effect of pile shape on observed heave.

Measurements of ground heave in front of a round pile in over-consolidated clay (Reese et al. 1968) are also shown in Figure 3-6 for comparison. In this case, the round pile had a diameter of 641 mm (25 inches). After a load of 596 kN (134 kips) was applied, heave measurements were taken up to 13 ft away from the pile. Considering the differences in pile diameter and soil type, the agreement with the data from this series of tests is remarkably good.
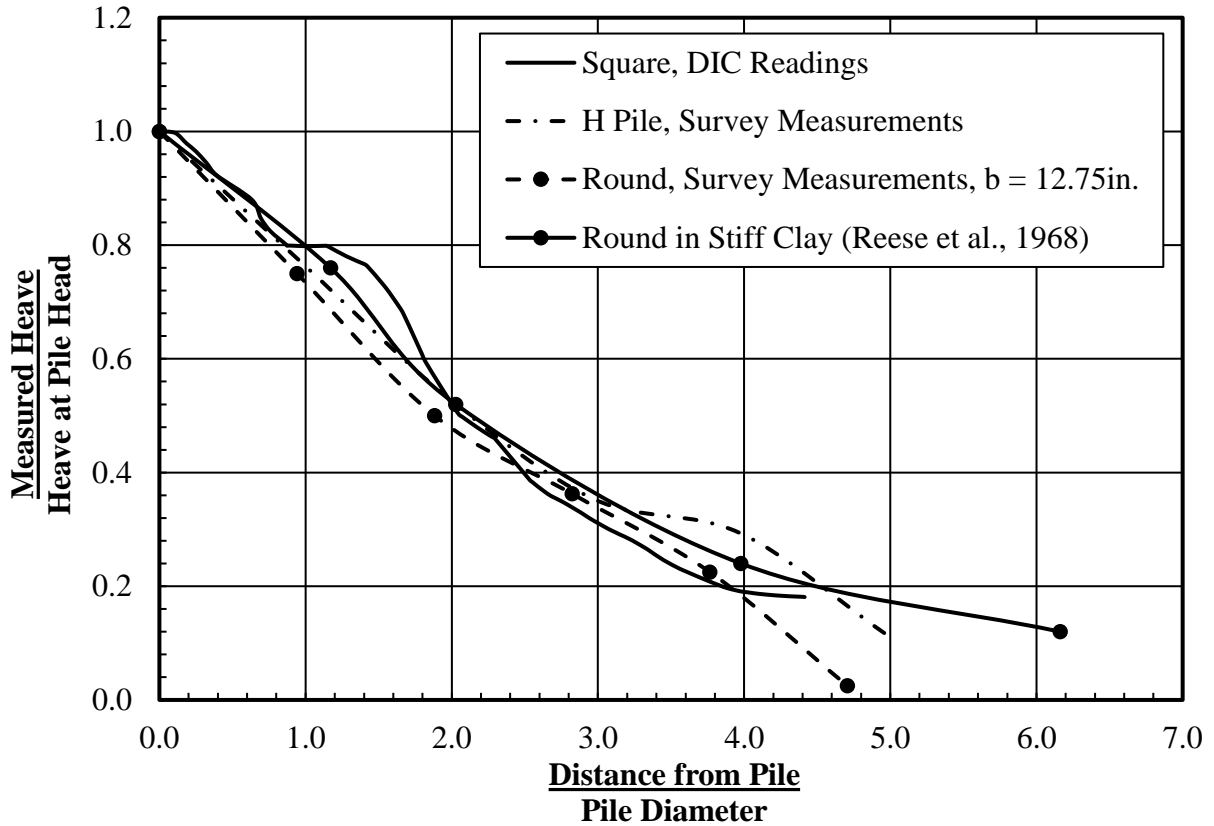
Figure 3-6: Normalized Ground Heave Measurements on square, round, and H piles

Apart from heave measurements, quantitative observations can be made from DIC contour plots created through the data analysis package, Istra-4D Q-400 (2014). Figure 3-7 and Figure 3-8 were created by assigning colors to various levels of displacement. The contour gradient ranges from cool to hot colors as initial displacements increase in magnitude. These image presents a representation of soil heave that could not be visually observed during testing. The color contours present the progression of the heave within the failure "wedge" or "bulb" surrounding the loaded pile. An analysis, similar to the heave plots shown previously, but in multiple directions from the pile allow further definition of the size of the stress bulb. DIC images were not available for the round pile.
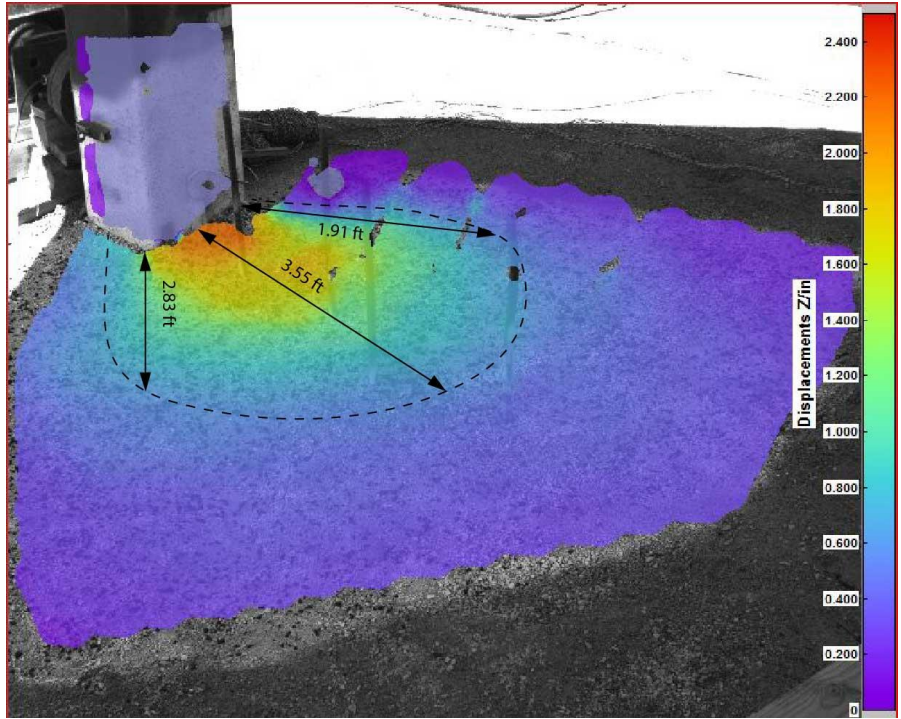
Figure 3-7: Vertical displacement contour plot for a square pile
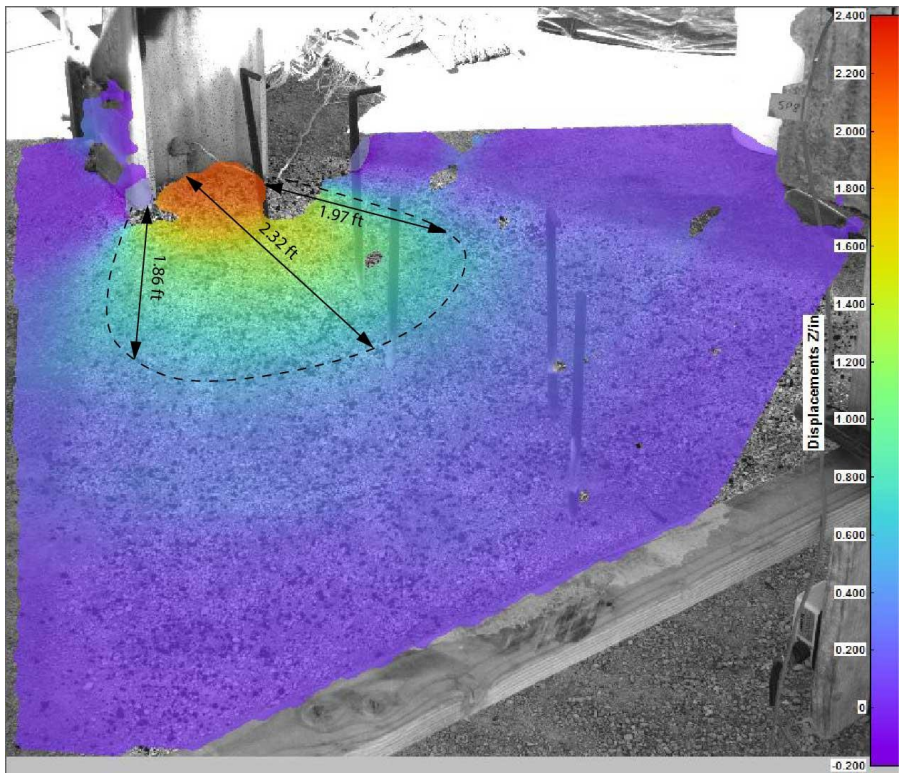
Figure 3-8: Vertical displacement contour plot for an H pile

26

Idealized stress bulbs have been shown on these images representing the boundary of 0.5 inches of vertical deflection. The stress bulb of the square and H pile reach 0.5 inch heave at 3.55 ft and 2.32 ft from the face, respectively. The magnitude of heave is shown on the legend at the right side of these figures as the hotter colors represent greater heave and cooler colors represent lower levels of heave. Going further from the pile the heave values eventually reach zero indicated by a purple color. Three-dimensional images, such as these, can be helpful in creating a more realistic model of the failure wedge.

4 LATERAL LOAD ANALYSIS

The purpose of this lateral load analysis was to develop a design approach or a model that accurately describes the lateral load contribution of square or H shaped piles. The accuracy of the approach can easily be evaluated by comparing the computed load-deflection curves with those measured during the lateral load tests. Close agreement between the two curves will indicate that the model produces the same results as observed in the load test. Three methods for considering the effect of pile shape were initially considered in this analysis, namely the equivalent diameter method proposed by Reese and Van Impe (2001), the shape factor approach suggested by Briaud et al. (1983), and a simple p-multiplier approach. The computer program LPILE (version 2015.8.03), developed by Ensoft, Inc., was chosen as a method of analysis due to its wide use in engineering practice and the versatility of the program in terms of pile behavior, soil behavior, and output options.

The soil models in LPILE were first calibrated by matching the computed load-deflection curves to the measured test data for the round piles assuming that behavior for this shape would be more accurately predicted. Subsequently, the same calibrated soil parameters were used to compute load-deflection curves for the square and H pile with the appropriate width and section modulus for each pile. Discrepancies between the measured and computed curves could then be attributed to differences in resistance associated with the pile shape. Finally, several approaches to account for the influence of pile shape on lateral resistance were used to determine if they could produce improved agreement with the measured behavior of the square and H pile.

The loads were applied in the program at a height of one foot above the ground surface using a pinned-head boundary condition to match field conditions. The granular backfill and native soil layers were both modeled using the p-y curve shape for sand developed by the API

(1982). In this approach, p is the horizontal soil resistance per length of pile and y is the lateral soil displacement. The API model requires data regarding the soil friction angle, ϕ; the lateral subgrade modulus, k; and moist unit weight, γ. The unit weight of the soil used was known from the density tests performed during construction; however, direct measurements of ϕ and k were not available. Thus, the friction angle, ϕ; and stiffness, k; were back-calculated with LPILE by matching the calculated load-deflection curves with those obtained from the field tests for the circular pile. Both friction angle and soil stiffness have an effect on the computed load-displacement curves; however, k has a greater effect on the curve at small deflections while ϕ has a greater effect on the curve at large deflection near the ultimate resistance.

In the calibration process, average measured load-deflection curves were used for the round piles in Phase 1 and 2 testing because the behavior was quite similar; however, a separate curve was required for the Phase 3 test because the soil was more compact. Soil properties used in the LPILE analysis for Phase 1 & 2 tests are provided in Table 4-1, while soil properties for Phase 3 tests are provided in Table 4-2. The load-deflection curves computed for the round piles using LPILE are compared with the measured curves in Figure 4-1 and the agreement is generally very good.

Table 4-1: Soil properties used in LPILE analysis for Phase 1 and 2 tests.

Soil Type	Depth (ft)	Moist Unit Weight, γ (lbs/ft^3)	Soil Friction Angle, ϕ (degrees)	Lateral subgrade modulus, k (lbs/in^3)
Compacted Gravelly Sand	0-15 (Phase 1) 0-20 (Phase 2)	129	45°	250
Native Silty Sand	15-33 (Phase 1) 20-38 (Phase 2)	125	34°	100

Table 4-2: Soil properties used in LPILE analysis for Phase 3 tests.

Soil Type	Depth (ft)	Moist Unit Weight, γ (lbs/ft^3)	Soil Friction Angle, ϕ (degrees)	Lateral subgrade modulus, k (lbs/in^3)
Compacted Gravelly Sand	0-6	131	51°	390
Compacted Gravelly Sand	6-20	129	45°	250
Native Silty Sand	20-38	125	34°	100

In modeling the square and H piles, the same soil properties were used as those used for the round pile; however, the appropriate width and moment of inertia were applied for each pile. The computed load-deflection curves are compared with the measured curves in Figure 4-2 for Phase 1 tests and the curves computed by LPILE generally underestimate the measured resistance from the field tests. At a load of 60 kips, the computed deflection for the square pile is about 0.30 inch greater than the measured deflection. Likewise, at a load of 60 kips the computed deflection for the H pile was 1.1 inches higher than the measured displacement. The discrepancy between the measured and computed curves suggests that the pile shape is producing greater soil resistance than would be expected based on a round pile shape.
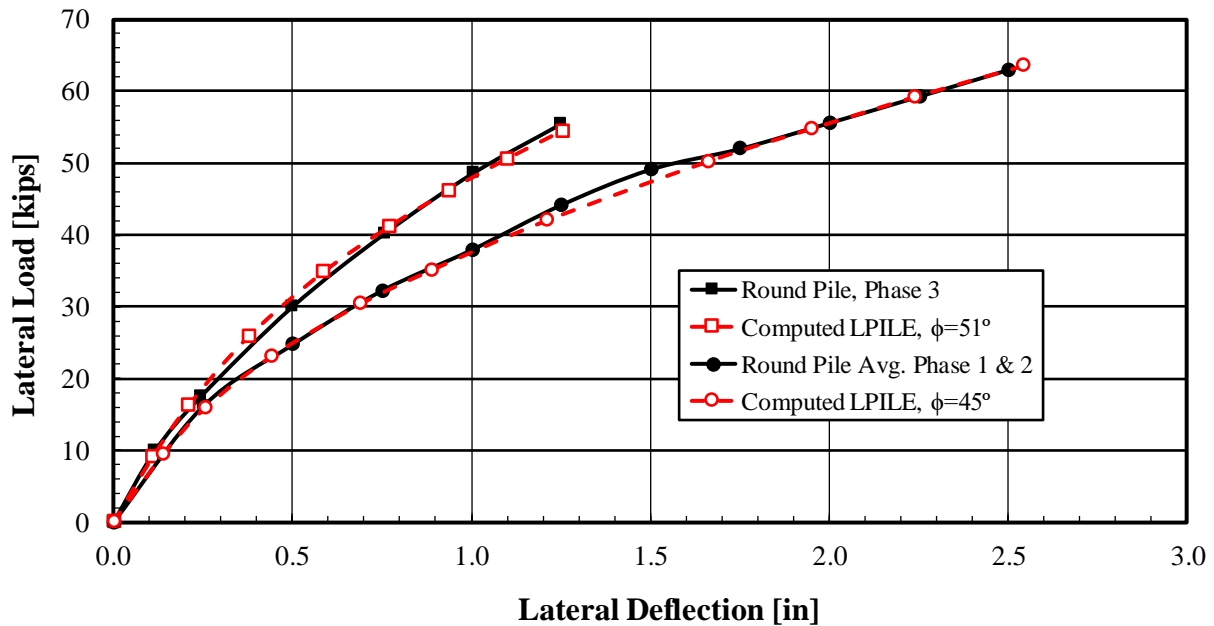
Figure 4-1: Comparison of computed load-deflection curves using LPILE with average measured curve for round piles in Phase 1 and 2 testing and Phase 3 testing.
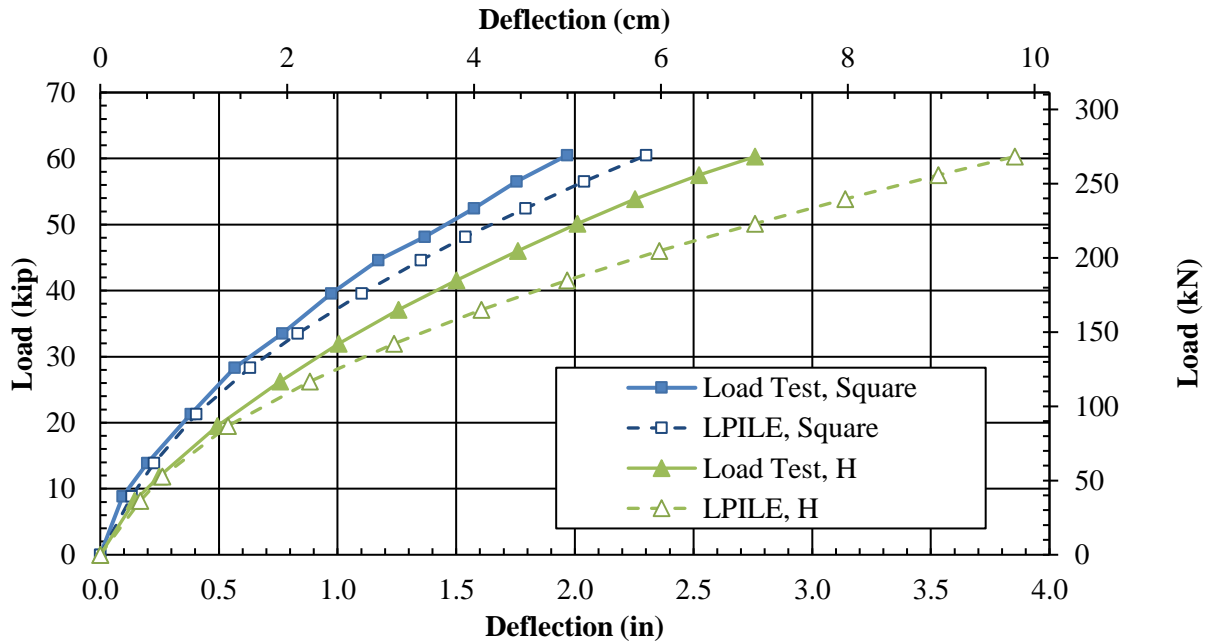

Figure 4-2: Comparison of the measured load-deflection curves for square and H piles with curves computed with the computer program LPILE using the same soil properties as used for the round pile in Phase 1 testing.

31

Reese and Van Impe (2001) proposed the use of an equivalent diameter to account for the increased lateral resistance on the sides of non-circular pile shapes. Unfortunately, this approach produced very little increase in the effective width, and the computed load-deflection curves were nearly the same as obtained when no correction was applied. The failure of this approach strongly suggests that the increased lateral resistance for the square and H piles is produced by an increase in both passive resistance and side shear resistance as suggested by Briaud et al (1983).

Briaud et al. (1983) developed a procedure for calculating passive resistance versus deflection (Q-y) and side shear resistance vs. deflection (F-y) curves at any depth along a pile. These two components could then be combined to produce a p-y curve that provides the overall lateral resistance of the pile. To account for pile shape, shape factors for round and square piles were proposed. To apply this approach, the p-y curves computed by LPILE for the round pile at each depth were computed and the F-y curves for a round pile was computed and subtracted from the p-y curves. The resulting Q-y and F-y curves were then multiplied by the ratio of the square to round shape factors to obtain the appropriate curves for a square pile. Finally, the Q-y and F-y curves were combined to give p-y curves which were manually input into LPILE for analysis. Although this approach provided better agreement with measured response, it was unable to consistently match the measured load-deflection curves and was very time consuming.

The p-multiplier approach is a simple and convenient method for adjusting the expected lateral soil resistance with the use of a modification factor. In the past, p-multipliers have been used to reduce the lateral soil resistance to account for pile group interaction from multiple rows of piles and to reduce lateral soil resistance in liquefied sand (Isenhower & Wang, 2015). Varying p-multipliers may be applied at any depth along the pile to account for stratified soil

32

layers of fluctuating strength. However, in this study, a simple constant p-multiplier was used along the entire pile length to account for the shape of the entire pile.

After applying p-multipliers to the square and H LPILE soil models, load vs. deflection curves were computed and plotted against the measured load vs. deflection curves from the load tests. For simplicity in comparison, the measured load vs. deflection curves for the H pile tests in Phase 1 and 2 were averaged into one curve. This simplification did not apply to the square piles due to the difference in soil compaction between phases 1 and 3. Therefore, separate p-multipliers were developed for the Phase 1 and Phase 3 tests. In all cases, the soil parameters obtained from the back-analysis of the appropriate companion round pile test were held constant in the p-multiplier analyses with the square and H piles. A simple trial and error approach was employed with multiple iterations using different p-multipliers until a computed load-deflection curve was developed that was very similar to the load-deflection curves for both the H and square piles. As shown in Figure 4-3, this analysis produced p-multipliers of 1.2 and 1.25 for the Phase 1 and Phase 3 square pile tests, respectively. The agreement between the computed curves and the measured load-deflection data (shown with markers) is very good in both cases. Considering the apparent difference in resistance between the two tests, the consistency in the back-calculated p-multipliers is also encouraging.

Figure 4-4 provides a plot of the computed load-deflection curve for the H pile in comparison with data points for the two H pile tests and the average curve. Once again the agreement between measured and computed response is very good with a p-multiplier of 1.2. The similarity between the back-calculated p-multipliers for the square and H piles provides further evidence that a reasonably consistent shape effect is being observed.
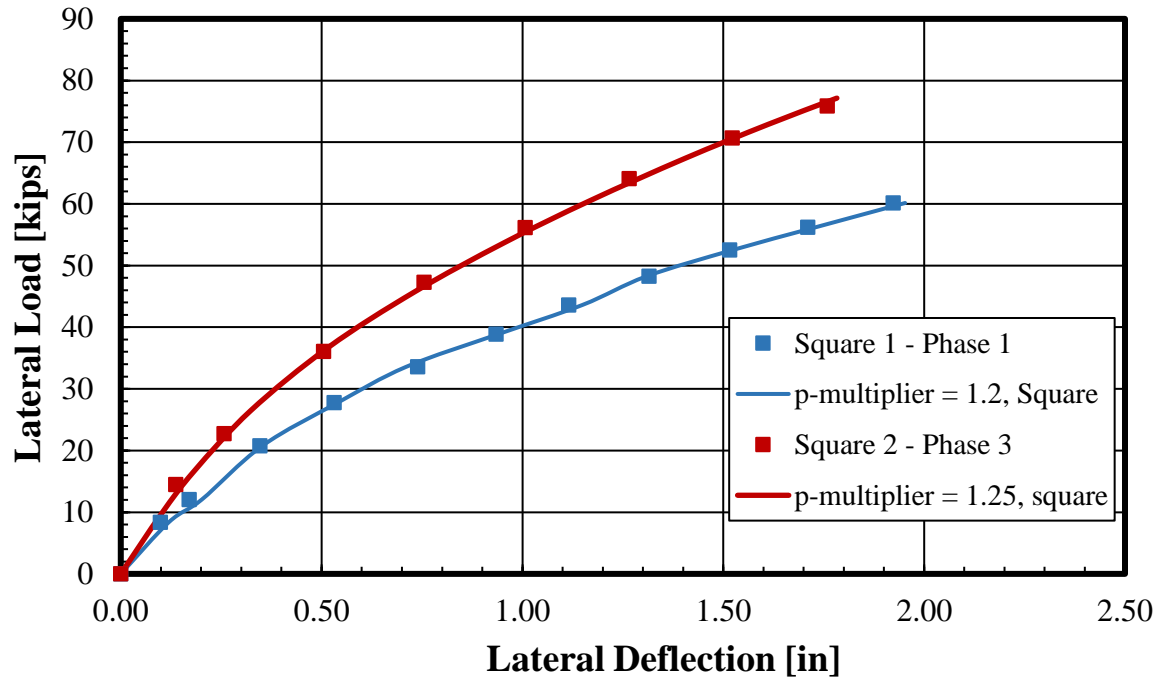
Figure 4-3: Load-deflection curves using the p-multiplier approach for square piles compared with measured load-deflection curves
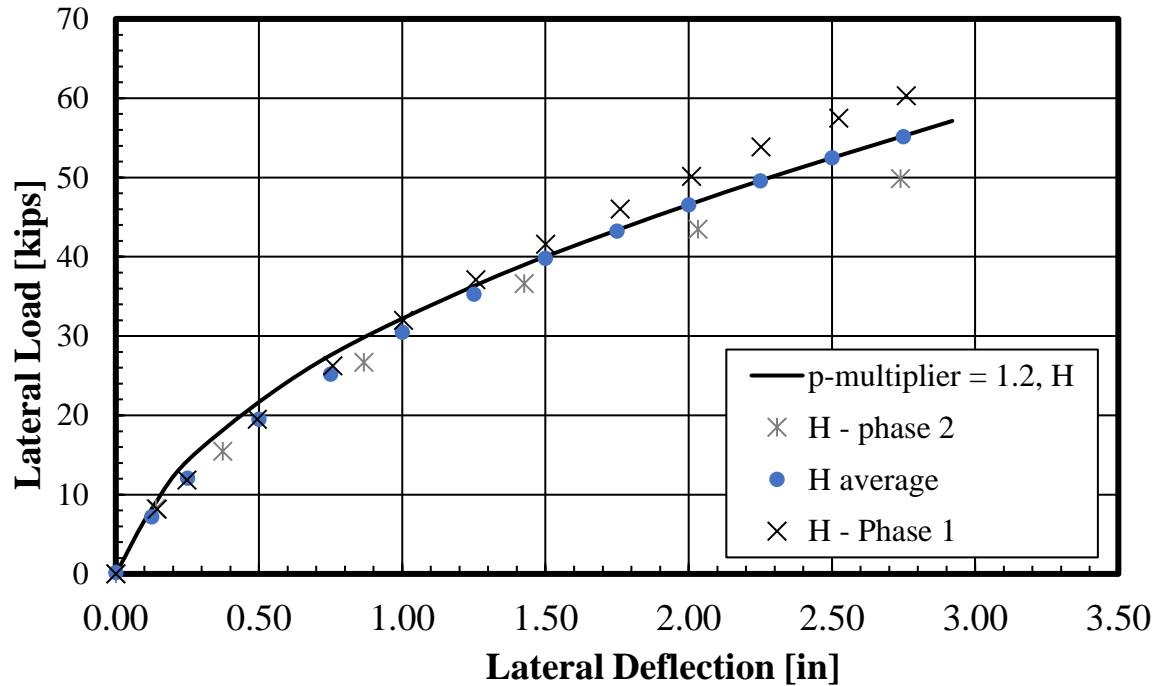

Figure 4-4: Load-deflection curves using the p-multiplier approach for H piles compared with measured load-deflection curves.

Along with the load deflection curves, agreement was also found between the moment versus depth measured by strain gauges and the calculated moment versus depth profiles produced by LPILE which ensures that the piles reacted similarly at all depths.

Based on the analysis of the full-scale load tests, it is recommended that a p-multiplier of 1.2 be use to account for shape effects for square and H piles when using analysis programs designed for round piles such as LPILE. These modification factors would account for the extra passive and side shear forces that square and H pile shapes provide. Using a p-multiplier of 1.2 for a pile implies that the combination of passive and shear forces around a square shaped pile provides a 20% increase in the lateral resistance provided by the soil relative to a round pile of comparable dimensions. The p-multiplier indicates that a square shaped pile can provide more capacity than what was estimated without regard to shape effect. This allows the full capacity of the pile to be appropriately considered in the design of deep foundations which has the potential to reduce foundation costs when lateral loads are an important consideration.

5 ADDITIONAL CONSIDERATIONS

A basic cost analysis can also provide insight on the whether or not the pile shape should be changed from a round to square pile shape for a given project. Apart from considering pile driving cost, the price of each pile can be correlated to its weight in steel. If each pile has similar material properties, then price per foot of pile is a ratio of the cross sectional area. This study utilized piles of comparable width and diameter. Although this similarity also extends to the cross sectional area of the square and the round piles, 14.8 in^2 and 14.57 in^2, respectively, the same cannot be said about the H pile with a cross-sectional area of 22.5 in^2. Using these factors as the basis of comparison, the square pile would cost 2% more than the round pile while the H pile, orientated about its weak axis, would cost 55% more than the round pile. This price can be reduced by using an H pile with a smaller section, such as a non-compact W12x53 shape, if bending capacity is not a large concern. As the price of steel is constantly fluctuating, these ratios will hold true in any market and other pile sizes with similar width/diameter and areas.

As demonstrated in this study, pile shape does have an influence on the lateral resistance of a pile. It has been shown that a square pile with a similar width, moment of inertia and cross sectional area as a round pile will provide more lateral resistance with nearly the same cost. An H pile on the other hand, oriented about the weak axis, will provide less resistance and possibly cost 55% more than a comparable round pile. Although pile shape is usually not the most important consideration in design, to the attentive engineer the use of pile shape factors can be an important factor that should be considered in the design of deep foundations.

Although a round pile and a square pile can provide similar moments of inertia in all directions, the moment of inertia for an H pile is significantly weaker in one direction than the other which can create problems in designing for some loads where the direction of force is not

known in advance. While both round and a square piles have the same moment of inertia in orthogonal directions, the reduction in side resistance due to a loss of contact with the soil will affect the round pile in both directions while full contact will be maintained with the square pile in both directions.

Both square and round piles with an end plate offer the potential for filling the hollow tube with reinforced concrete which can significantly increase the composite moment of inertia and moment capacity of the section. Of course, this opportunity is not provided by an H pile.

Lastly, round piles and square piles with end-plates are displacement piles which generate high excess pore pressure when driven in clays while H piles are low-displacement piles which "cookie-cut" through the clay and generate relatively low pore pressures. Experience has shown that displacement piles can cause consolidation over time which leads to an increase in axial side resistance relative to non-displacement piles. For example, Rollins (2008) performed axial uplift load tests on a round pile and an H pile driven in a clay profile in Salt Lake City, Utah five months after driving. Although the H pile had a larger perimeter than the round pile, the round pile yielded a much higher uplift capacity than the H pile. The unexpected increase in resistance was attributed to consolidation around the round pile after driving the displacement pile.

In addition to the increased lateral resistance provided by square piles relative to the round and H piles, the additional factors discussed previously indicate that a square pile might be beneficial to employ for a number of other reasons.

6   CONCLUSIONS

1. As theorized by several investigators, full-scale lateral load tests demonstrate that the lateral resistance of square and H piles is greater than that for round piles after accounting for differences in widths and moments of inertia.

2. Back-analysis of full-scale tests indicates that a p-multiplier of 1.2 can provide reasonable agreement with measured lateral load vs. deflection curves and bending moment vs depth curves for square and H piles. A p-multiplier of 1.2 implies that the combination of passive and shear forces acting on a square shaped pile provides a 20% increase in the lateral resistance provided by the soil relative to a round pile of comparable width. The p-multiplier approach is simple and convenient for use with existing analysis programs.

3. Square piles have approximately the same moment of inertia in all directions similar to a round pile; however, an H pile provides considerably less lateral resistance when oriented about its weak axis particularly in comparison to a square pile because of its lower moment of inertia.

4. Increasing the effective width of a square pile to account for increased side resistance as suggested by Reese and Van Impe (2001) was insufficient to account for the increased lateral resistance.   The failure of this approach also suggests that increased passive resistance on the front face of a square pile is also a major contributor to the increased lateral resistance.

5. Methods which account for shape effects on side shear and passive resistance as suggested by Briaud et al (1983) show promise but are presently more inconsistent and time-consuming than the simple p-multiplier approach.

6. Shear planes for the square and H piles were distinct and flared out linearly from the edges of the front face in contrast to those for the round pile where shear planes were more diffused and the failure surface was more elliptical.

7. The horizontal ground displacement with distance from the pile face show similar trends for laterally loaded piles of different shapes. Normalizing the results showed that at a distance of five pile diameters from the pile face the soil only experienced about 10% of the lateral deflection at the pile face.

8. The vertical ground displacement or heave can be reasonably predicted in front of a pile using normalized relationships. These trends appear to be similar for different pile shapes and match test results in stiff clay as well. At a distance from the pile of four pile diameters, the soil experiences less than 25% of the vertical heave at the face of the pile.

REFERENCES

American Petroleum Institute, (2010). *Recommended Practice for Planning, Designing and Constructing Fixed Offshore Platforms - Working Stress Design, API RP 2A-WSD*, 21st Edition, Errata and Supplement, 2010.

Briaud, J.L., Smith, T.D., and Meyer, B. (1983). "Laterally Loaded Piles and the Pressuremeter: Comparison of Existing Methods", ASTM STP 983.

Bustamante, G. (2014). "Influence of Pile Shape on Resistance to Lateral Loading", MS Thesis, Department of Civil and Environmental Engineering, Brigham Young University, Provo, UT.

Coduto, D. P. (2001). Foundation Design: Principles and Practices. Prentice Hall, Upper Saddle River, NJ.

Duncan, J. M., Evans, L. T., and Ooi, P. S. K. (1994). "Lateral Load Analysis of Single Piles and Drilled Shafts." *Journal of Geotechnical Engineering*, 120(5), 1018–1033.

Filz, G. M., Arenas, A. E., Cousins, T. E., (2013). "Thermal Response of Integral Abutment Bridges with Mechanically Stabilized Earth Walls" *VCTIR 13-R7*.

GOOGLE EARTH (2015) "Test Site." 40°27'14.08" N and 111°53'53.60" W. Sampled December 20, 2015.

Isenhower, W.M., Wang S. (2015). "Technical Manual for LPILE 2015 (Using Data Format Version 8)", Ensoft Inc., Austin, TX.

Isenhower, W.M., Wang S. (2015). "User's Manual for LPILE 2015 (Using Data Format Version 8)", Ensoft Inc., Austin, TX.

"Istra-4D Q-400." (2014). computer software, Dantec Dynamics, Skovlunde, Denmark.

Reese, L. C., and Van Impe, W. F. (2001), "Single Piles and Pile Group under Lateral Loading", A. A. Balkema, Rotterdam, Netherlands.

Reese, L.C., W.R. Cox & F.D. Koop (1968). Lateral load tests of instrumented piles in stiff clay at Manor, Texas. A report to Shell Development Company, 303 pp. (published).

Rollins, K.M., Russell, D.N., and Bustamante, G. (2018). "The Influence of Pile Shape and Pile Sleeves on Lateral Load Resistance in Sand", *Utah Department of Transportation, Report No. UT-18.15.*

Russell, D. N. (2016). "The Influence of Pile Shape and Pile Sleeves on Lateral Load Resistance." MS Thesis, Civil & Environmental Engineering Dept., Brigham Young University, Provo, UT.

Smith, T. D., (1987), "Side Friction Mobilization F-y Curves for Laterally Loaded Piles from the Pressuremeter," *Prediction and Performance in Geotechnical Engineering: Proceedings of the International Symposium*, p. 89-95, Calgary, June 1987.